Effect of an Organoclay on the Reaction-Induced Phase-Separation Kinetics and Morphology of a Poly(ether imide)/Epoxy Mixture

Mao Peng, Dasong Li, Ying Chen, Qiang Zheng

Department of Polymer Science and Engineering, Zhejiang University, Hangzhou, 310027, China

Received 26 December 2005; accepted 3 November 2006
DOI 10.1002/app.25759
Published online in Wiley InterScience (www.interscience.wiley.com).

ABSTRACT: Organically modified layered silicates with a hydroxyl-substituted quaternary ammonium surfactant as the modifier were incorporated into a mixture of poly (ether imide) and epoxy with 4,4′-diaminodiphenyl sulfone as the hardener. The influence of the organically modified layered silicates on the reaction-induced phase-separation kinetics and morphology of the poly(ether imide)/epoxy mixture was investigated with time-resolved small-angle light scattering, phase-contrast microscopy, and scanning electron microscopy. The phase-separation kinetics were analyzed by means of the temporal evolution of scattering vector $\mathbf{q_m}$ and scattering intensity I_m at the scattering peak. The organically modified layered silicates obviously facilitated an earlier onset of phase separation but reduce the phase-separation rate and greatly retarded the domain-coarsening process in the late stage of spinodal decomposition. The temporal evolution of both $\mathbf{q_m}$ and I_m followed the power law $\mathbf{q_m} \sim (t - t_{os})^{-\alpha}$ and $I_m \sim (t - t_{os})^{-\beta}$, where t is the reaction time, t_{os} is the onset time of phase separation, and α and β are growth exponents. For the samples filled with organically modified layered silicates, α crossed over from 0 to about 1/3, following Binder–Stauffer cluster dynamics, and an interconnected phase structure was observed for cure temperatures ranging from 120 to 230°C. For the unfilled samples, the interconnected phase structure was observed only at cure temperatures below 140°C. At temperatures above 150°C, α crossed over from 0 to 1/3 $< \alpha \leq 1$ under the interfacial tension effect, following Siggia's theory, and the domain-coarsening rate was very fast; this resulted in macroscopic epoxy-rich domains. © 2007 Wiley Periodicals, Inc. J Appl Polym Sci 104: 1205–1214, 2007

Key words: light scattering; morphology; phase separation

INTRODUCTION

Reaction-induced phase separation in mixtures of thermosets and thermoplastics is a very important physical/chemical phenomenon in polymer science.[1] Typical examples include mixtures of epoxy and thermoplastics such as reactive liquid rubbers,[2] poly (methyl methacrylate),[3] poly(phenylene oxide),[4] poly (ether sulfone),[5] poly(phenylene ether),[6] poly(ether imide) (PEI),[7] polysulfone,[8] poly(ε-caprolactone),[9] polyimide,[10] and some copolymers.[11] It has been widely accepted that the final mechanical properties of these mixtures are determined by the phase structure. Generally, an interconnected or bicontinuous phase-separated microstructure with fine domain sizes benefits the properties because both the toughness of the thermoplastics and the stiffness of the thermosetting matrix can be combined in the final products. Therefore, the morphology evolution, phase-separation kinetics, and interaction between them have always been the focus in the study of reaction-induced phase separation.

Recently, thermoplastic and thermosetting nanocomposites filled with organically modified layered silicates (OLSs), that is, organoclays, have attracted great interest because of their remarkably improved thermal stability, impact resistance, gas-barrier properties, flammability resistance,[12] and other physical and mechanical properties at relatively low filler contents. The intercalation and exfoliation behavior of organoclays in polymer matrices and the final properties of the nanocomposites have been extensively investigated. However, as far as we know, little attention has been paid to the influence of organoclays on the phase structure and reaction-induced phase-separation behavior of thermosetting/thermoplastic mixtures.

Furthermore, previous studies have indicated that some fillers, including microscopic particles and fibers, have an important influence on the phase-separation behavior of binary polymer blends, especially when the fillers show selective (preferential) wettability to one component of the mixtures. The dynamic coupling between the wetting and phase-separation processes strongly affects the morphology evolution. For example, Turmel and Partridge[13] investigated the heterogeneous phase-separation phe-

Correspondence to: M. Peng (pengmao@zju.edu.cn).
Contract grant sponsor: National Natural Science Foundation of China; contract grant numbers: 50203013, and 20574060.

nomenon of epoxy/PEI blends around glass, carbon, and aramid fibers. It was found that a discrete epoxy-rich layer formed around the glass fibers, whereas no such layer was observed around the carbon and aramid fibers. This was due to the preferential wettability of epoxy to the glass fiber and indicated that the surface properties of the fillers had a strong impact on the morphology evolution of reaction-induced phase separation. Lipatov et al.[14] found that fumed silica affected the phase-separation temperatures and kinetics of poly(methyl methacrylate)/poly(vinyl acetate) blends. At a shallow quench depth, the phase-separation rate of the filled blends was much slower than that of the unfilled blends, and the activation energy was also lower. Tanaka[15] found that microscopic glass particles greatly affected the pattern evolution of mixtures of a styrene oligomer and ε-caprolactone. Glass particles were preferentially included in the more wettable phase, and the growth rate of spinodal decomposition (SD) diminished as either the particle concentration was increased or their diffusivity decreased. Karim and coworkers[16] found that the presence of filler particles led to the development of circular composition waves (target patterns) about the filler particles during the intermediate stage of phase separation. Microscale silica particles could lower the consulate temperature of low-molecular-weight polystyrene (PS) and polybutadiene blends when they interacted attractively with one component of the blends.[16] More recently, Krishnamoorti et al.[17] investigated in detail the influence of organoclay on the phase-separation behavior of PS/poly(vinyl methyl ether) (PVME) blends and found that the phase-separated structure was of a smaller length scale than that of the unfilled blends. All these studies indicate that both microsize and nanosize fillers can strongly affect the phase-separation behavior of binary polymer mixtures. However, to the best of our knowledge, most researchers have focused their attention on the influence of microsize particles on the isothermally induced phase separation of thermoplastic mixtures, but little attention has been paid to the influence of nanoparticles on the reaction-induced phase-separation kinetics and morphology of thermoplastic/thermoset mixtures.

In this study, we selected a ternary mixture of PEI, epoxy, and organoclay as a model system to investigate the influence of nanofillers on the reaction-induced phase-separation kinetics and the final morphology of the nanocomposites with time-resolved small-angle light scattering (TR-SALS), phase-contrast microscopy (PCM), and scanning electron microscopy (SEM). The filler particles in our study were preferentially wettable with the epoxy oligomer because a hydroxyl-substituted quaternary ammonium surfactant reactive with the epoxy was used as the modifier for the OLS. The phase-separation kinetics were analyzed in detail by means of the temporal evolution of scattering vector $\mathbf{q_m}$ and scattering intensity I_m at the scattering peak. It is shown that both the $\mathbf{q_m}$ and I_m values follow the power law $\mathbf{q_m} \sim (t - t_{os})^{-\alpha}$ and $I_m \sim (t - t_{os})^{-\beta}$, where t is the reaction time, t_{os} is the onset time of phase separation, and α and β are growth exponents.

EXPERIMENTAL

Materials

Liquid diglycidyl ether of bisphenol A (DGEBA) type epoxy with an epoxide equivalent weight (i.e., the weight in grams of the epoxy resin that contained 1 g equiv of epoxides) of 194–198 g/equiv and an average molecular weight of 392 g/mol was purchased from Heli Resin Co., Ltd. (Suzhou, China). Methylene dichloride and 4,4′-diaminodiphenyl sulfone (DDS) were from China Medicine Group (Shanghai, China). The PEI used in this study was GE Ultem 1000 (GE Plastics, Pittsfield, MA) (number-average molecular weight = 26,000 g/mol, weight-average molecular weight = 50,000 g/mol). OLS (commercial brand C18OH-Mt) was acquired from Zhejiang Huate Chemical Co., Ltd. (Hangzhou, China). The intercalated spacing (d_{001}) of the pristine OLS was about 1.96 nm. After it was mixed with the epoxy oligomer, d_{001} became 3.68 nm, and after curing, it became larger where parts of the OLS were exfoliated. C18OH-Mt was treated with a hydroxyl-substituted quaternary ammonium modifier, which afforded the flexibility to combine the catalytic functionality with the enhanced miscibility of OLS toward epoxy. The chemical structures of the cationic surfactant in C18OH-Mt and other chemicals are presented in Figure 1. All the chemicals and resin were used as received.

Sample preparation

Both filled and unfilled mixtures were prepared. The OLS powder was dried *in vacuo* for more than 24 h at 80°C before sample preparation. DGEBA (5.0 g) and 1.4 g of PEI were weighed and dissolved in methylene dichloride. For the OLS-filled sample, 0.6 g of OLS was dispersed in the solution, and this was followed by fierce stirring and sonication for several minutes to obtain uniform suspensions. The solutions and suspensions were then placed in a circulation oven at room temperature for more than 3 days to remove most of the solvent and then placed in a vacuum oven at 100°C to remove the residual solvent. Subsequently, a stoichiometric amount of DDS (31.7 parts by weight per 100 parts by weight of DGEBA) was added to the mixture and

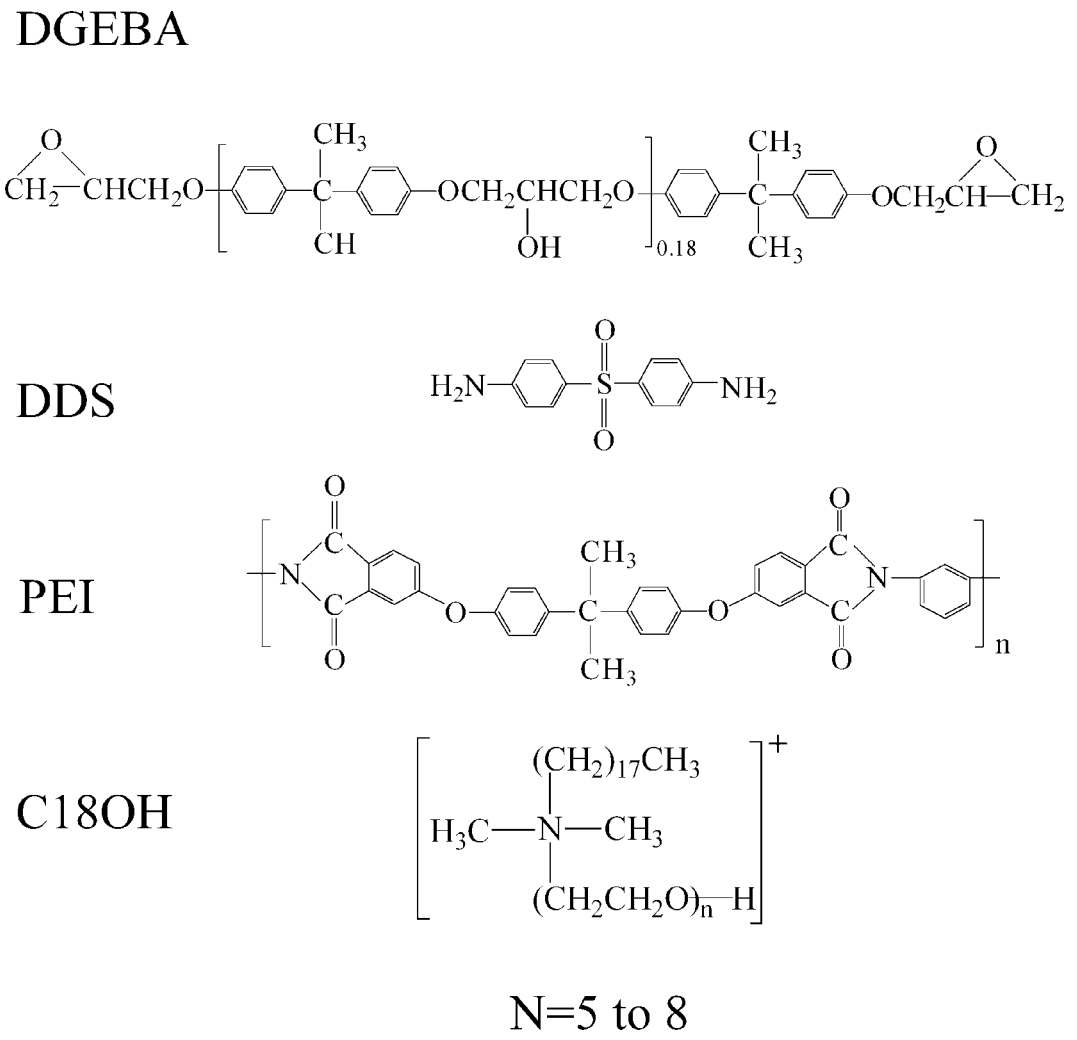

Figure 1 Chemical formulas for DGEBA, DDS, PEI, and C18OH-Mt.

stirred for 5–6 min at 140°C until it dissolved in the mixture completely.

PCM

The samples were sandwiched between two microscope glass cover slides and pressed into thin films with a thickness of about 30 μm on a hot stage preheated to 90°C for PCM observation. Thin aluminum foil was used to control the sample thickness. The specimens were then placed on the hot stage preheated to various temperatures (from 120 to 230°C) and isothermally cured. The morphology was observed on a phase-contrast microscope (Motic B1-220PH, Motic China, Xiamen, China), and the images were recorded with a digital camera (Coolpix 4500, Nikon, Tokyo, Japan) with a resolution of 1.9 megapixels.

Electron microscopy

After being cured at various temperatures for different times, the samples were fractured in liquid nitrogen, placed in methylene chloride, and stirred for more than 48 h to make sure that PEI was completely removed. The samples were then coated with gold and characterized by SEM (JSM-5510LV, JEOL, Ltd., Tokyo, Japan) at a voltage of 20 kV. Because it was difficult to complete the cure reaction under temperatures below 180°C, the samples were further postcured at 180°C for another 2 h. We found that if the curing reaction was not completed, the samples swelled after being placed in methylene dichloride, so the morphology observed by SEM would be different. At the same time, postcuring could not affect the morphology of these samples because of their sufficient gelation or vitrification before postcuring.

TR-SALS

Similarly to those in the PCM experiments, the thin sample films were obtained via hot pressing on the hot stage preheated to 90°C. The sample films without OLS were transparent and clear. The samples filled with OLS were almost optically clear with a

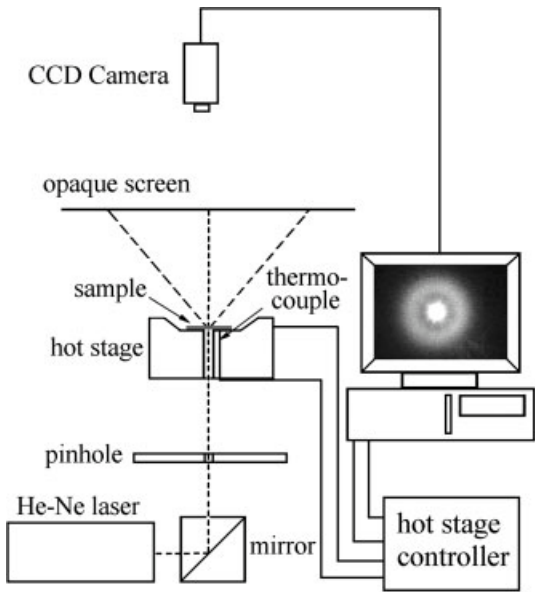

Figure 2 Schematic illustration of the SALS apparatus.

faint blue tint, which resulted from the refractive-index difference (RID) between OLS and the PEI/epoxy matrix. OLS increased the scattering light slightly at the beginning of the experiments. Furthermore, during phase separation, OLS potentially aggregated in the epoxy-rich phase, so the influence of OLS on the scattering light could be more complicated. However, as discussed in the following sections, the scattering light caused by the phase separation between epoxy and PEI was very strong, so the influence of OLS on the scattering light was neglected in this study. A laboratory-made TR-SALS apparatus, as reported in many previous studies,[18] was employed to investigate the curing-induced phase-separation behavior of the hybrid nanocomposites in this study. Figure 2 presents a schematic illustration of the small-angle light scattering (SALS) apparatus. A He–Ne laser generator with a power of 3 mW (Optical Instruments Plant, Zhejiang University, Hangzhou, China) was used as the light source. The wave number of the He–Ne laser was 632.8 nm. The laser beam was reflected by a prism and became vertical. The hot stage had a power of 100 W and was controlled by an intelligent controller (AI-700, Yuguang, Xiamen, China). The scattering light impinged on an opaque screen and formed the scattering pattern, which was recorded in real time by a charged-coupling-device camera (MTV-1802CB, Mintron, Taiwan, China) at appropriate time intervals, and then imported into the computer memory through a video capturing board (Video Vesa, Daheng, Beijing, China). Subsequently, the relationship between the scattering intensity and the scattering vector was obtained by online circular averaging of the intensity of the radial symmetric scattering pattern.

Differential scanning calorimetry (DSC) analysis

The dynamic curing behavior of the filled and unfilled mixtures was investigated with a differential scanning calorimeter (Pyris 1, PerkinElmer, Fremont, CA) at a heating rate of 10°C/min under the protection of nitrogen. The temperature increased from 80 to 340°C. The weight of the samples was about 5–8 mg. The degree of chemical conversion (X_c) was calculated with the following equation:

$$X_c = \frac{\Delta H_T}{\Delta H_{\text{total}}} \tag{1}$$

where ΔH_T is the heat released up to temperature T, obtained by the integration of the calorimetric signal up to that temperature, and ΔH_{total} is the total reaction heat associated with the complete conversion of all reactive groups.

RESULTS AND DISCUSSION

Morphology

Figure 3 presents the PCM micrographs of the unfilled and filled PEI/epoxy mixtures cured at various temperatures. The domain size and morphology of the unfilled samples (A1–A10) are strongly affected by the cure temperature. At temperatures below 140°C (A1–A4), an interconnected phase structure, or in other words, a co-continuous morphology, can be observed. With the cure temperature increasing, the domain size increases, and the morphology is altered significantly. At cure temperatures between 150 and 190°C (A5–A9), an inverted phase structure can be observed, in which the PEI-rich minor phase is continuous, whereas the epoxy-rich major phase is interrupted. This phenomenon results from the dynamic asymmetry and the apparent domain coarsening under the interfacial tension effect at the late stage of phase separation. Furthermore, when the cure temperature increases from 150 to 190°C, both the shape and phase domain size change significantly. The epoxy-rich domains turn from irregular to more and more spherical, and the domain size apparently increases. At 180 and 190°C, some epoxy-rich domains are about 100 μm with a spherical or oval shape. As is well known, with the temperature increasing, the mixture viscosity decreases and domain coarsening becomes more rapid; therefore, the domains transform into the shape of lowest interfacial energy (sphere) with a much larger size under the driving of interfacial tension. At cure temperatures above 190°C, the PEI-rich domains shrink rap-

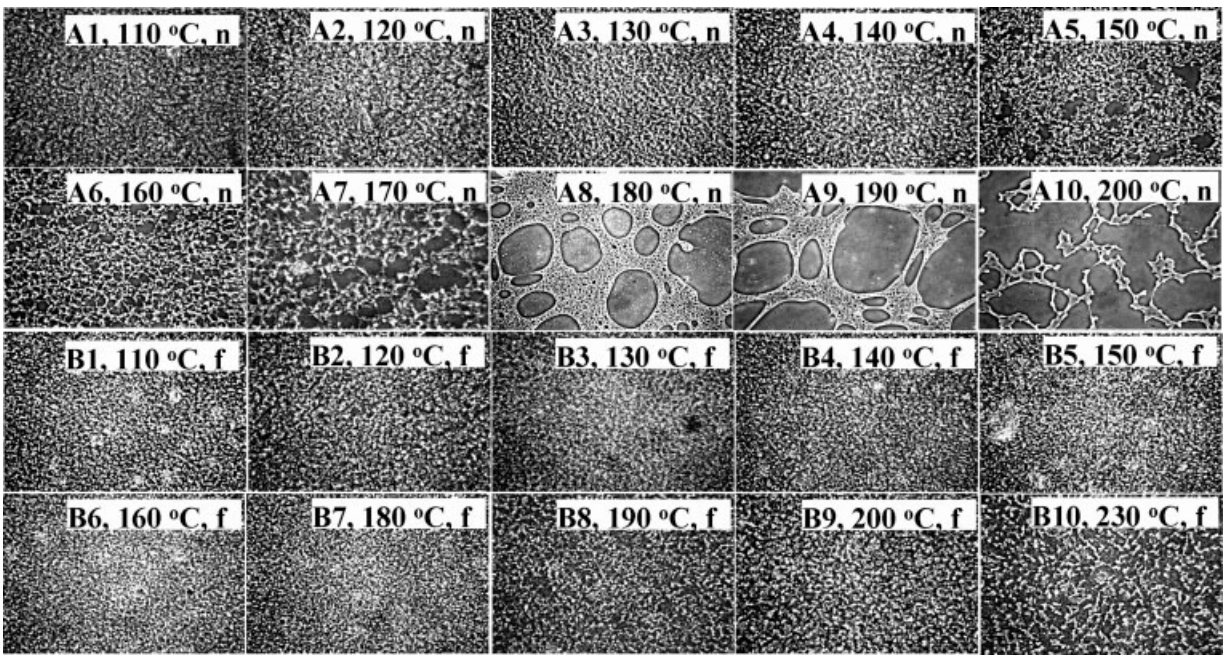

Figure 3 PCM images (original magnification = 400×) for (A1–A10) PEI/DGEBA/DDS (*n* means that the samples were not filled) and (B1–B10) PEI/DGEBA/DDS/OLS mixtures (*f* means that the samples were filled with OLS) cured at various cure temperatures.

idly and interrupt into broken threads under the interfacial tension effect at the late stage of SD, and the epoxy-rich domains become interconnected again.

On the contrary, the influence of the cure temperature on the morphology and domain size of the filled specimens [Fig. 3(B1–B10)] is quite limited. AN interconnected phase structure can be observed in all the samples, regardless of the cure temperature. The inverted phase structure for the dynamically asymmetric epoxy/thermoplastic mixtures cannot be observed in these filled samples. Furthermore, the domain size increases gradually with the increase in the cure temperature, but no macroscopically spherical phase domains like that in the unfilled samples cured at temperatures above 150°C can be observed.

Figure 4(A,B) presents the SEM morphology of the fractured surface of the unfilled samples at the cure temperatures of 120 and 150°C, respectively. The interconnected phase structure at 120°C is obvious, and the size of the epoxy-rich domains is increased greatly at 150°C. Figure 4(C,D) presents the SEM micrographs of the filled samples cured at 120 and 210°C, respectively. The interconnected phase structure can be observed for both cases. The average domain size at 210°C is only slightly larger than that at 120°C. The SEM observation indicates that all the filled samples at cure temperatures ranging from 120 to 210°C exhibit an interconnected phase structure similar to that in Figure 4(C,D), and the domain size increases only gradually with the cure temperature. This is consistent with what has been observed by PCM.

On the basis of these experimental results, one can conclude that the incorporation of OLS strongly depresses the domain coarsening, prevents the formation of macroscopic phase domains, and facilitates the formation of an interconnected phase structure.

As previously mentioned, in studying the phase-separation behavior of glass-particle-filled mixtures of a styrene oligomer and ε-caprolactone, Tanaka[15] found that the morphology was determined by the particle density. At a low particle density, a droplet structure was observed, whereas an interconnected structure was observed when the particle density was high enough, because the glass spheres assembled into an ordered structure with hexagonal packing, and the spontaneous pinning effect of the ordered glass particles significantly retarded the domain-coarsening process. On the other hand, many authors[19] have investigated the influence of OLS on the viscoelasticity of the OLS-filled nanocomposites of different polymer matrices. The zero shear viscosity of the nanocomposites increases apparently with an increase in the clay content. On the basis of these experiments, it is reasonable to speculate that the thin silicate platelets in the polymer matrix form interconnected networks as the result of the intercalation and exfoliation of OLS during the cure reaction. Because of the preferential wettability of epoxy to OLS, epoxy-rich phase domains form around the OLS particles, and this results in an interconnected structure. Under the spontaneous pinning effect, the domain-coarsening rate is obviously reduced, and the interconnected structure remains.

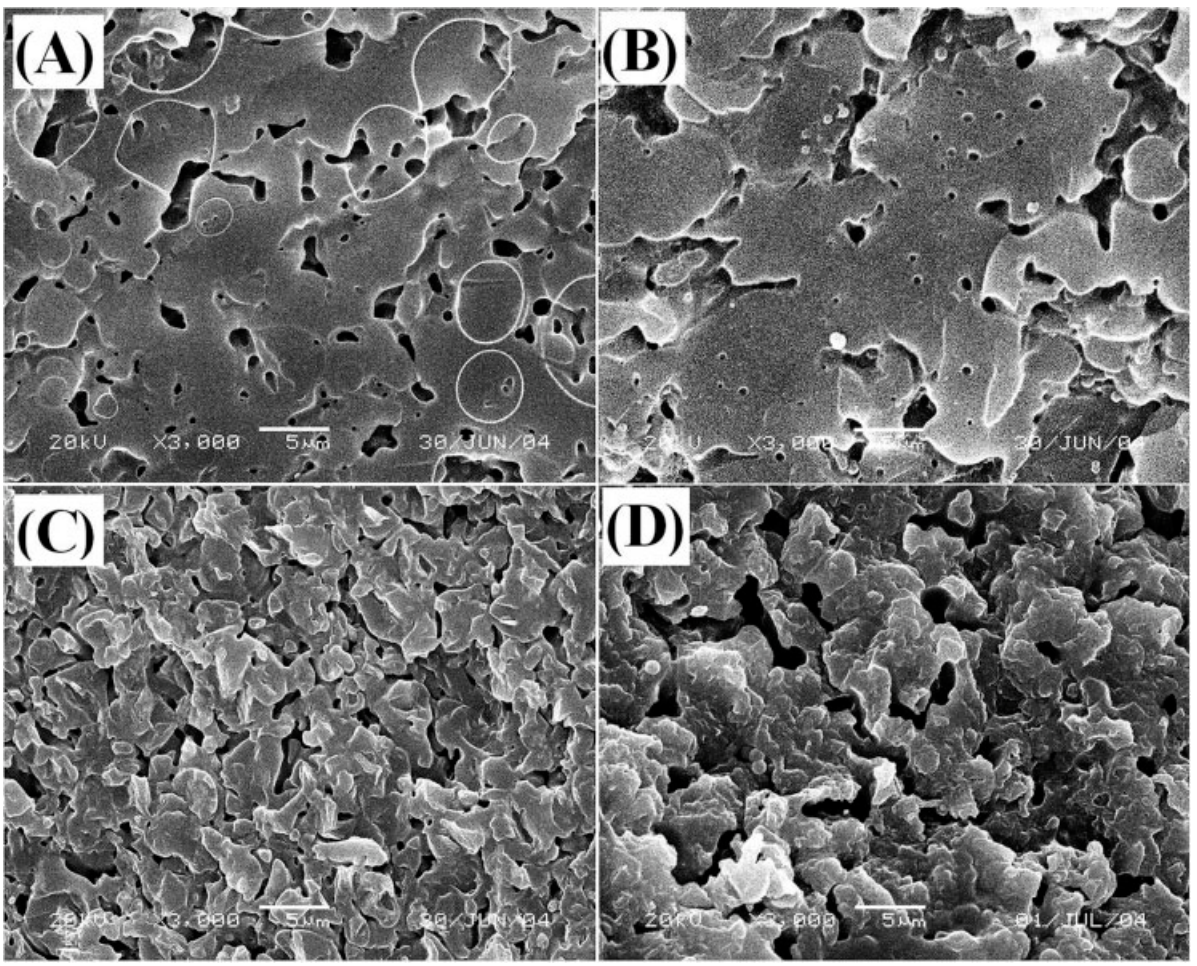

Figure 4 SEM images (original magnification = 3000×) of PEI/DGEBA/DDS mixtures at cure temperatures of (A) 120 and (B) 150°C and of PEI/DGEBA/DDS/OLS mixtures at cure temperatures of (C) 120 and (D) 210°C.

This is further discussed in the following section on the basis of the SALS data.

Phase-separation mechanism

Reaction-induced phase separation in epoxy/thermoplastic mixtures usually follows the SD mechanism. Figure 5 gives the typical temporal evolution of the scattering profiles for the filled specimens cured at 170°C. The definition of the scattering vector is $\mathbf{q} = 4\pi n/\lambda \sin(\theta/2)$, where θ, λ, and n are the scattering angle, the wavelength of the laser light, and the refractive index of the medium ($n = 1$ for light scattering measurements conducted in air), respectively. Clear scattering halos can be observed at all cure temperatures ranging from 120 to 210°C. Furthermore, in the early stage of phase separation, the $\mathbf{q_m}$ values are invariant, and the scattering intensity keeps on increasing, following the characteristic of SD. Also, as mentioned previously, the interconnected phase structure observed by PCM and SEM indicates that the reaction-induced phase separation of the filled mixtures follows the SD mechanism. It is possible that the OLS particles act as nucleation agents during phase separation because the C18OH-Mt-modified OLS has preferential wettability to

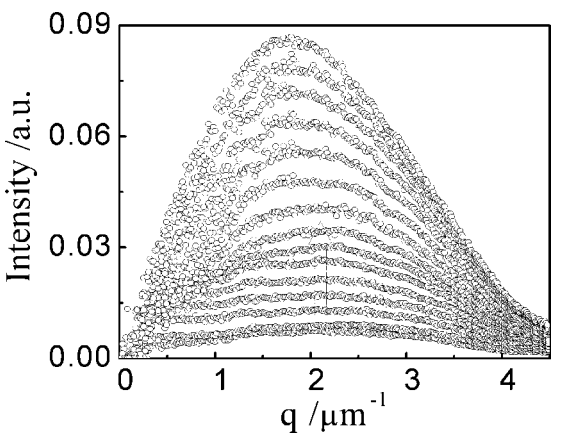

Figure 5 Temporal evolution of the scattering intensity profiles for PEI/DGEBA/DDS/OLS mixtures at the cure temperature of 170°C.

epoxy, but no evidence of nucleation and growth phase separation has been observed in our study.

Phase-separation kinetics

Temporal evolution of $\mathbf{q_m}$ and I_m

During reaction-induced phase separation, the chemical reaction and the physical phase-separation processes are combined. The chemical reaction starts from the very beginning of the experiment, but the system is miscible in the early period of the reaction, and no phase separation occurs until the molecular weight of epoxy increases to a certain value at which the system becomes immiscible. Therefore, the onset of phase separation is behind that of the cure reaction. We now consider the phase-separation kinetics according to the temporal evolution of $\mathbf{q_m}$ and I_m.

Figure 6 presents the temporal evolution of $\mathbf{q_m}$ and I_m values for the filled and unfilled specimens at various curing temperatures. Obviously, the filled samples exhibit earlier onsets of phase separation. Also, at cure temperatures above 150°C, the $\mathbf{q_m}$ values of the filled samples decrease less rapidly, and their I_m values increase less rapidly than those of unfilled samples. Therefore, OLS brings about an earlier phase separation but reduces the rate of phase separation.

Figure 7(A) presents the DSC dynamic scans of the filled and unfilled samples at the heating rate of 10°C/min. The exothermic peaks representing the progression of the cure reaction can be observed for both specimens. Both the onset temperature and peak temperature in the exothermic curve of the filled sample, denoted by the arrows, are lower than those of the unfilled sample, and this indicates that OLS can accelerate the cure reaction. Figure 7(B) presents the relationship between the cure temperature and the degree of conversion. It is clear that the cure reaction of the filled specimen is faster than that of the unfilled specimen. This is consistent with what has been reported previously for other OLS/epoxy systems and confirms that the protonated alkyl ammonium cation has a catalytic effect on the cure reaction of epoxy.[12(a,b)] The earlier onset of phase separation of the filled specimens, as shown in Figure 6, should be the result of the faster cure reaction.

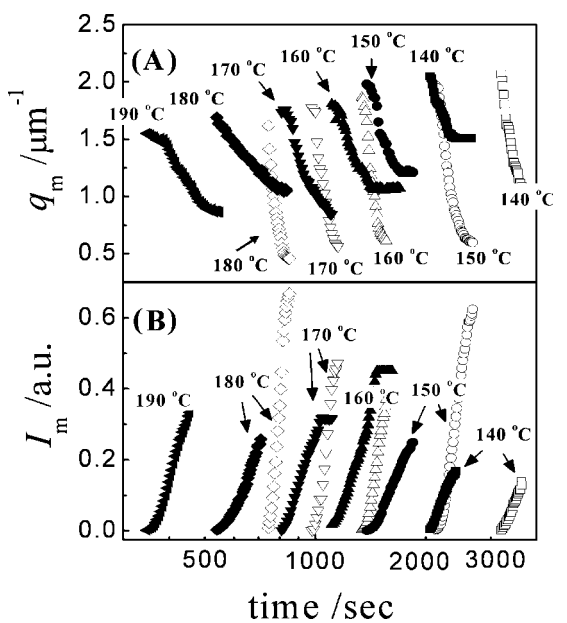

Figure 6 Temporal evolution of (A) $\mathbf{q_m}$ and (B) I_m for unfilled samples (hollow symbols) and filled samples (solid symbols) at cure temperatures of (■,□) 140, (●,○) 150, (▲,△) 160, (▼,▽) 170, (◆,◇) 180, and (◀) 190°C.

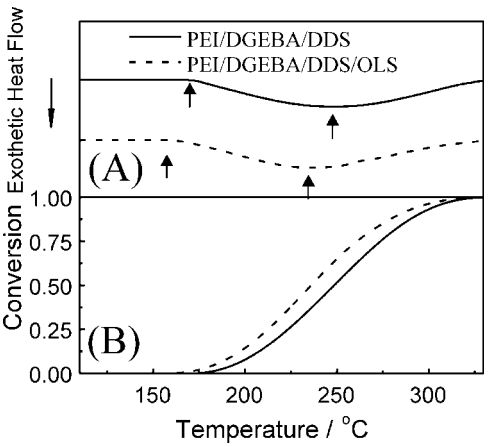

Figure 7 (A) Dynamic DSC scans and (B) relationship between the cure temperature and the degree of conversion for the DGEBA/PEI/DDS/OLS and DGEBA/PEI/DDS mixtures at a heating rate of 10°C/min under the protection of nitrogen.

The final $\mathbf{q_m}$ values of the filled specimens are higher than those of the unfilled specimens. Because Λ_m, the wavelength of composition fluctuation, or in other words, the periodic distance of the phase-separated structure, is inversely proportional to $\mathbf{q_m}$, following $\Lambda_m = 2\pi/\mathbf{q_m}$, the final average domain size of the unfilled specimens is larger than that of the filled specimens. This indicates that domain coarsening of the filled specimens is greatly diminished as the result of OLS incorporation.

Power-law behavior of $\mathbf{q_m}$ and I_m

We now consider the power-law behavior of $\mathbf{q_m}$ and I_m in the reaction-induced phase separation of the PEI/DGEBA/DDS and PEI/DGEBA/DDS/OLS mixtures. As is well known, during isothermally induced SD, the temporal evolution of domain growth follows the simple power law $\mathbf{q_m} \sim t^{-\alpha}$ and $I_m \sim t^{\beta}$. The values of growth exponents α and β are determined

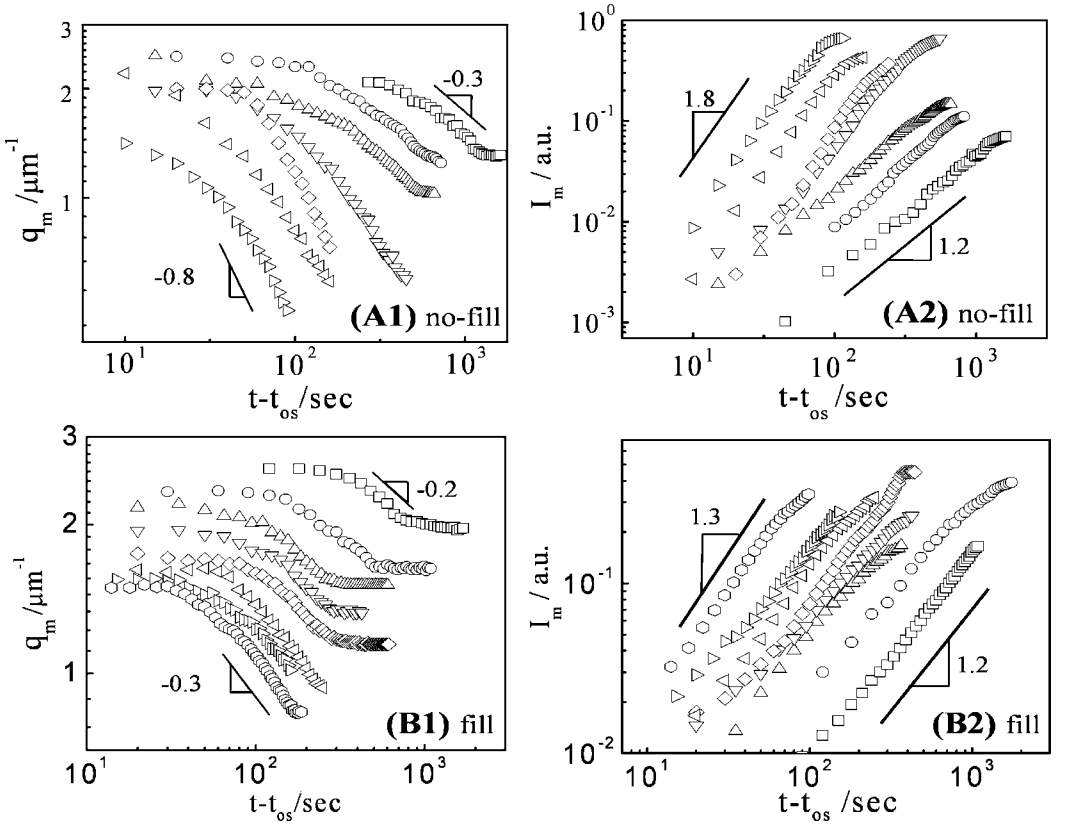

Figure 8 Curves of log $\mathbf{q_m}$ versus log($t - t_{os}$) and log I_m versus log($t - t_{os}$) for (A1,A2) unfilled and (B1,B2) filled samples at cure temperatures of (□) 120, (○) 130, (△) 140, (▽) 150, (◇) 160, (◁) 170, (▷) 180, and (⬡) 190°C.

by the mechanism controlling the domain growth. When the domain growth is controlled by the diffusive mechanism, α crosses over from 1/6 to 1/3,[20] and at the later stage of SD, the interfacial tension effect results in a crossover of $\alpha = 1/3$ to $\alpha = 1$ (viscosity-controlled).[21] In the intermediate regime of SD, the relationship between α and β follows $\beta > 3\alpha$ for the phase separation in the three dimensions. At the late stage of SD, the concentration fluctuations reach equilibrium, and the relationship between α and β follows $\beta = 3\alpha$.

The applicability of this power law has been confirmed by both experimental observations and theoretical simulations[22] for thermally induced phase separation by many researchers, but, as mentioned previously, during reaction-induced phase separation, there exists an induction time, namely, a period before the onset of phase separation. During the induction time, the specimens are still homogeneous, and no phase separation occurs. Therefore, we believe that the induction time should be subtracted from the total reaction time when we use the power law to analyze the phase-separation dynamics. If we denote the onset of phase separation as t_{os}, the power law should be modified into the following form: $\mathbf{q_m} \sim (t - t_{os})^{-\alpha}$ and $I_m \sim (t - t_{os})^{\beta}$. The value of t_{os} for various cure temperatures can be easily determined as the time at which I_m appears and starts to increase abruptly (Fig. 6). On the other hand, during the reaction-induced phase separation, the molecular weight of the system increases with time. It should be emphasized that the phase separation in the epoxy/thermoplastic mixture is very fast compared with the chemical reaction. For example, one can find in Figure 6 that it takes about 20 min for the DGEBA/DDS/PEI mixture to reach gelation or vitrification at 170°C, but it takes less than 3 min to complete the phase separation; therefore, the increase in the molecular weight during the phase-separation process should be very limited.

Figure 8 presents the double logarithmic plots of $\mathbf{q_m}$ and I_m values against ($t - t_{os}$) for the filled and unfilled mixtures at cure temperatures ranging from 120°C to 190°C.

First, let us discuss the general features of the curves of log $\mathbf{q_m}$ versus log($t - t_{os}$) and log I_m versus log($t - t_{os}$). In Figure 8(A1,A2), we can find that, at relatively low cure temperatures, the curves of log $\mathbf{q_m}$ versus log($t - t_{os}$) can be obviously divided into three stages for both the filled and unfilled specimens. In the initial region, the $\mathbf{q_m}$ values are invariant, indicating that the phase-separation structure

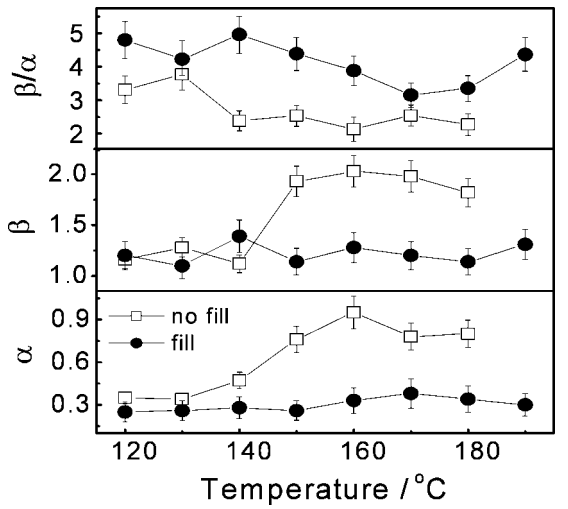

Figure 9 α, β, and β/α values for filled samples (solid symbols) and unfilled samples (hollow symbols) at various cure temperatures.

has a fixed spatial wave number of the concentration fluctuation, following the characteristics of the early stage of SD. Then, the log $\mathbf{q_m}$ values decrease gradually. Satisfactory linear sections can be observed in the curves of log $\mathbf{q_m}$ versus log($t - t_{os}$) for all the samples. The slope of this section is defined as the α value. Then, in the third stage, the log $\mathbf{q_m}$ values become nearly invariant with time again as the result of the occurrence of gelation or vitrification of the system. At higher cure temperatures, gelation or vitrification cannot be observed because the average domain size is too large and the corresponding $\mathbf{q_m}$ value is too small to be determined accurately. As for the curves of log I_m versus log($t - t_{os}$), it can be found in Figure 8(B1,B2) that, for all the samples, the main parts of these curves exhibit satisfactory linearity. After the occurrence of gelation or vitrification, log I_m keeps on increasing with smaller slopes. After gelation or vitrification, the refractive index of epoxy keeps on increasing with the curing reaction; therefore, RID between the two phases keeps on increasing. Because the scattering intensity is positively proportional to the RID of the system, the I_m values continue to increase.

Because the linear sections can be observed in the curves of log $\mathbf{q_m}$ versus log($t - t_{os}$) and log I_m versus log($t - t_{os}$), we believe that the power law is applicable to the reaction-induced phase-separation behavior of our system. The α, β, and β/α values for the filled and unfilled samples at various cure temperatures are presented in Figure 9.

We now discuss in detail the influence of the cure temperature on the kinetics of reaction-induced phase separation and its relationship with the morphology evolution. The α and β values for the unfilled samples are more sensitive to the cure temperature than those for OLS-filled samples. As can be found in Figures 8(A1) and 9, at temperatures below 140°C, the α values are about 1/3, the β values are close to 1, and the β/α ratio is close to 3, indicating the applicability of the Binder–Stauffer theory, according to which α changes from 1/6 for the intermediate stage of SD to 1/3 for the late stage of SD. This phenomenon is also consistent with the experimental observations of the PS/polymethylphenylsiloxane mixture[23] and the PS/PVME mixture.[24]

However, at temperatures above 150°C, α crosses over rapidly to 0.7–1.0 soon after the initial stage of phase separation, which is close to Siggia's prediction for the late stage of SD. The β values increase to about 2.0, indicating that hydrodynamics plays an important role in domain coarsening. According to Siggia's calculation, $\alpha = 1$, $\beta = 3$, and $\beta/\alpha = 3$ for hydrodynamics-controlled SD at the late stage. However, the β/α values for our samples are smaller than 3. This phenomenon is related to the dimensionality. The specimens sandwiched between two glass slides are thin films with a thickness of about 30 μm. Therefore, phase separation occurs in two dimensions, resulting in $\beta/\alpha \approx 2$. In summary, at relatively high cure temperatures, the interfacial tension effect plays an important role in determining the final phase structure of the unfilled samples and results in higher α and β values. The SALS result is consistent with that of the PCM observation. As mentioned previously, large macroscopic phase domains can be observed in the unfilled samples at cure temperatures above 150°C. This obviously results from the apparent domain coarsening under the interfacial tension effect at the late stage of SD.

On the contrary, for the OLS-filled specimens, the influence of the cure temperature on the α and β values are quite limited. When the cure temperature increases from 120 to 190°C, the α and β values for the main linear sections of curves of log $\mathbf{q_m}$ versus log($t - t_{os}$) and log I_m versus log($t - t_{os}$) are around 1/3 and 1, respectively. As mentioned previously, for the unfilled samples, no macroscopic phase domains could be observed through PCM. This indicates that there is a strong pinning effect of the nanofillers in the filled samples, and the domain-coarsening procedure is greatly diminished. It can also be found that the β/α values for the filled samples are relatively high. According to Takeno and Hashimoto,[22(c)] the relationship between α and β follows $\beta > 3\alpha$ at the intermediate stage of SD and $\beta = 3\alpha$ at the late stage of SD. Therefore, the fact that the β values of the filled samples are larger than 3α indicates that the phase-separation rate of the filled samples is relatively slow, and it is difficult for these samples to reach the late stage of SD before the occurrence of gelation or vitrification.

CONCLUSIONS

The influence of OLS on the reaction-induced phase-separation behavior of a PEI/epoxy mixture was studied with SALS, PCM, and SEM over a wide range of cure temperatures. OLS greatly affected the phase-separation behavior. The onset of phase separation was earlier, but the phase-separation rate was reduced, and domain coarsening at the late stage of SD was greatly diminished; this resulted in an interconnected phase structure with a fine domain size at cure temperatures even above 190°C. This is in contrast with the fact that unfilled PEI/epoxy mixtures have an interconnected phase morphology only at cure temperatures below 150°C. Moreover, the reaction-induced phase separation of PEI/epoxy/OLS mixtures follows the simple power law of $\mathbf{q_m} \sim (t - t_{os})^{-\alpha}$ and $I_m \sim (t - t_{os})^{\beta}$. At cure temperatures above 140°C, growth exponent α crosses over from 0 to a high value ($1/3 < \alpha \leq 1$) under the interfacial tension effect, and macroscopic phase domains appear. On the contrary, the α values of the filled samples cross over from 0 to about 1/3 for all cure temperatures ranging from 120 to 230°C, indicating that the existence of nanofillers strongly diminishes interfacial-tension-accelerated domain coarsening.

References

1. Inoue, T. Prog Polym Sci 1995, 20, 119.
2. (a) Fröhlich, J.; Thomann, R.; Mülhaupt, R. Macromolecules 2003, 36, 7205; (b) Lee, H. S.; Kyu, T. Macromolecules 1990, 2, 459; (c) Bussi, P.; Ishida, H. J Polym Sci Part B: Polym Phys 1994, 32, 647.
3. Cabanelas, J. C.; Serrano, B.; Baselga, J. Macromolecules 2005, 3, 961.
4. Wu, S. J.; Lin, T. K.; Shyu, S. S. J Appl Polym Sci 2000, 75, 26.
5. (a) Kim, B. S.; Chiba, T.; Inoue, T. Polymer 1995, 36, 43; (b) Pethrick, R. A.; Hollins, E. A.; McEwan, I.; MacKinnon, A. J.; Hayward, D.; Cannon, L. A.; Jenkins, S. D.; McGrail, P. T. Macromolecules 1996, 15, 5208.
6. (a) Lestriez, B. J.; Chapel, P.; Gérard, J. F. Macromolecules 2001, 34, 1204; (b) Chao, H. S. I.; Whalen, J. M. J Appl Polym Sci 1993, 9, 1537.
7. (a) Giannotti, M. I.; Foresti, M. L.; Mondragon, I.; Galante, M. J.; Oyanguren, P. A. J Polym Sci Part B: Polym Phys 2004, 21, 3953; (b) Riccardi, C.; Borrajo, J.; Williams, R. J. J.; Girard-Reydet, E.; Sautereau, H.; Pascault, J. P. J Polym Sci Part B: Polym Phys 1996, 2, 349; (c) Gan, W.; Yu, Y.; Wang, M.; Tao, Q.; Li, S. Macromolecules 2003, 36, 7746.
8. (a) Oyanguren, P. A.; Aizpurua, B.; Galante, M. J.; Riccardi, C. C.; Cortázar, O. D.; Mondragon, I. J Polym Sci Part B: Polym Phys 1999, 19, 2711; (b) Park, S. J.; Kim, H. C. J Polym Sci Part B: Polym Phys 2001, 1, 121.
9. (a) Chen, J. L.; Chang, F. C. Macromolecules 1999, 32, 5348; (b) Chen, J. L.; Chang, F. C. Polymer 2001, 5, 2193.
10. Cho, J. B.; Hwang, J. W.; Cho, K.; An, J. H.; Park, C. E. Polymer 1993, 34, 4832.
11. (a) Rebizant, V.; Venet, A.-S.; Tournilhac, F.; Girard-Reydet, E.; Navarro, C.; Pascault, J. P.; Leibler, L. Macromolecules 2004, 21, 8017; (b) Barral, L.; Cano, J.; Díez, F. J.; López, J.; Ramírez, C.; Abad, M. J.; Ares, A. J Polym Sci Part B: Polym Phys 2002, 3, 284.
12. (a) Kong, D.; Park, C. E. Chem Mater 2003, 15, 419; (b) Becker, O.; Cheng, Y.-B.; Varley, R. J.; Simon, G. P. Macromolecules 2003, 36, 1616; (c) Koerner, H.; Hampton, E.; Dean, D.; Turgut, Z.; Drummy, L.; Mirau, P.; Vaia, R. Chem Mater 2005, 8, 1990; (d) Brown, J. M.; Curliss, D.; Vaia, R. A. Chem Mater 2000, 11, 3376; (e) Miyagawa, H.; Rich, M. J.; Drzal, L. T. J Polym Sci Part B: Polym Phys 2004, 23, 4384; (f) Miyagawa, H.; Rich, M. J.; Drzal, L. T. J Polym Sci Part B: Polym Phys 2004, 42, 4391; (g) Lü J.; Ke, Y.; Qi, Z.; Yi, X. J Polym Sci Part B: Polym Phys 2001, 39, 115; (h) Guo, B.; Ouyang, X.; Cai, C.; Jia, D. J Polym Sci Part B: Polym Phys 2004, 42, 192; (j) Triantafillidis, C. S.; LeBaron, P. C.; Pinnavaia, T. J. Chem Mater 2002, 14, 4088.
13. Turmel, D. J. P.; Partridge, I. K. Compos Sci Technol 1997, 57, 1001.
14. Nesterov, A. E.; Lipatov, Y. S.; Horichko, V. V.; Iganatova, T. Macromol Chem Phys 1998, 199, 2609.
15. Tanaka, H. Phys Rev Lett 1994, 16, 2581.
16. (a) Karim, A.; Douglas, J. F.; Nisato, G.; Liu, D.; Amis, E. J. Macromolecules 1999, 32, 5917; (b) Karim, A.; Liu, D. W.; Douglas, J. F.; Nakatani, A. I.; Amis, E. J. Polymer 2000, 41, 8455.
17. (a) Yurekli, K.; Karim, A.; Amis, E. J.; Krishnamoorti, R. Macromolecules 2003, 36, 7256; (b) Yurekli, K.; Karim, A.; Amis, E. J.; Krishnamoorti, R. Macromolecules 2004, 37, 507.
18. (a) Kyu, T.; Saldanha, J. M. Macromolecules 1988, 21, 1021; (b) Edel, V. Macromolecules 1995, 28, 6219; (c) Peng, M.; Yuan, X. X. Macromol Chem Phys 2004, 205, 256.
19. (a) Lee, K. M.; Han, C. D. Macromolecules 2003, 36, 7165; (b) Maiti, P. Langmuir 2003, 19, 5502; (c) Brown, J. M.; Curliss, D.; Vaia, R. A. Chem Mater 2000, 12, 3376.
20. Binder, K.; Stauffer, D. Phys Rev Lett 1973, 33, 1006.
21. Siggia, E. D. Phys Rev A 1979, 20, 595.
22. (a) Kyu, T.; Saldanha, J. M. Macromolecules 1988, 21, 1021; (b) Lee, H.; Kyu, T.; Gadkari, A.; Kennedy, J. P. Macromolecules 1991, 24, 4852; (c) Takeno, H.; Hashimoto, T. J Chem Phys 1998, 15, 1225; (d) Chen, H.; Chakrabarti, A. J Chem Phys 1998, 108, 6006.
23. Kuwahara, N.; Sato, H.; Kubota, K. Phys Rev E 1993, 47, 1132.
24. (a) Hashimoto, T.; Itakura, M.; Shimidzu, N. J Chem Phys 1986, 85, 6773; (b) Izumitani, T.; Takenaka, M.; Hashimoto, T. J Chem Phys 1990, 92, 3213.